

Torben Koenigk · Uwe Mikolajewicz · Helmuth Haak
Johann Jungclaus

Variability of Fram Strait sea ice export: causes, impacts and feedbacks in a coupled climate model

Received: 21 December 2004 / Accepted: 11 July 2005 / Published online: 8 November 2005
© Springer-Verlag 2005

Abstract Analyses of a 500-year control integration of the global coupled atmosphere–sea ice–ocean model ECHAM5.0/MPI-OM show a high variability in the ice export through Fram Strait on interannual to decadal timescales. This variability is mainly determined by variations in the sea level pressure gradient across Fram Strait and thus geostrophic wind stress. Ice thickness anomalies, formed at the Siberian coast and in the Chukchi Sea, propagate across the Arctic to Fram Strait and contribute to the variability of the ice export on a timescale of about 9 years. Large anomalies of the ice export through Fram Strait cause fresh water signals, which reach the Labrador Sea after 1–2 years and lead to significant changes in the deep convection. The associated anomalies in ice cover and ocean heat release have a significant impact on air temperature in the Labrador Sea and on the large-scale atmospheric circulation. This affects the sea ice transport and distribution in the Arctic again. Sensitivity studies, simulating the effect of large ice exports through Fram Strait, show that the isolated effect of a prescribed ice/fresh water anomaly is very important for the climate variability in the Labrador Sea. Thus, the ice export through Fram Strait can be used for predictability of Labrador Sea climate up to 2 years in advance.

surface salinity, which is due to melting and freezing of sea ice. The ice export through Fram Strait is by far the largest export of ice out of the Arctic. It amounts to about 2,400–3,200 km³/year (ca 75,000 to 100,000 m³/s) (Vinje et al. 1998; Vinje 2001; Schmith and Hansen 2003; Aagaard and Carmack 1989). The interannual variability is mainly controlled by the annual mean sea level pressure gradient across Fram Strait. According to Vinje (2001) and Hilmer et al. (1998), the pressure gradient explains more than 80% of the variability. Brümmer et al. (2003) pointed out that single cyclones could lead to substantial ice export as well. Results of Arfeuille et al. (2000) indicate the importance of ice thickness for the ice export. Venegas and Mysak (2000) performed a frequency singular value decomposition of sea ice concentration and sea level pressure (SLP) from 1903 to 1994 north of 40°N. They found three significant peaks in the ice export, at 6–7, 9–10 and 16–20 years. Hilmer and Lemke (2000) and Polyakov and Johnson (2000) showed variability in Arctic sea ice dynamics with a timescale of about 10–12 years. This is consistent with the anticyclonic and cyclonic regime with both persisting for about 5–7 years as proposed by Proshutinsky and Johnson (1997). Mysak and Venegas (1998) suggested a 10-year climate cycle in the Arctic, which should be characterised by a clockwise propagation of sea ice anomalies through the Arctic and SubArctic and a coexisting standing oscillation in SLP anomalies. With its high variability, the ice export through Fram Strait is crucial for convection in the Labrador Sea, and thus for the entire thermohaline circulation. Dickson et al. (1988) and Belkin et al. (1998) suggested that the great salinity anomaly (GSA) in the Labrador Sea in the beginning of the 1970s was caused by large positive anomalies in the ice export through Fram Strait. This signal propagated in the East Greenland Current to the south, melted and flew as a fresh water anomaly into the Labrador Sea. Häkkinen (1999) used idealised fresh water pulses in the East Greenland Current to simulate this process. Her model reproduced the observed salinity anomalies in the Labrador Sea and the decrease in oceanic convection. In

1 Introduction

The northern Polar Sea and the Nordic Seas play a substantial role in the climate system. A large amount of the oceanic deep-water masses is formed there. This occurs in the direct vicinity to strong gradients in the sea

T. Koenigk (✉) · U. Mikolajewicz · H. Haak · J. Jungclaus
Max-Planck-Institut für Meteorologie,
Bundesstr. 53, 20146 Hamburg, Germany
E-mail: kahl@dkrz.de
Tel.: +49-40-41173280
Fax: +49-40-41173298

the simulation, it took several years until the convection in the Labrador Sea recovered. Haak et al. (2003) concluded from simulations with the ocean model MPI-OM (Marsland et al. 2003) that the GSA's in the 1980s and 1990s were caused by anomalous large ice exports through Fram Strait as well. These findings confirm results from Koeberle et al. (1999).

Furthermore, the ice export through Fram Strait has a considerable effect on the ice cover in the Greenland Sea (Walsh and Chapman 1990) and can lead to large and long-lasting anomalies. The advective character of this process modifies the close local connection between direct atmospheric forcing and sea ice variability (Wang and Ikeda 2000; Dickson et al. 2000).

Observational analysis from Deser et al. (2000) suggests a northward shift in the storm track as consequence of low ice concentration in the Greenland Sea. SLP is decreased as result of enhanced heat fluxes from ocean to atmosphere in the areas of reduced sea ice.

Recently, Magnusdottir et al. (2004) and Deser et al. (2004) investigated the effects of North Atlantic sea surface temperature and sea ice anomalies on the winter circulation in the CCM3 atmospheric circulation model. They used 40-year trends that were observed in sea ice and SST to derive a realistic spatial pattern of the anomalous forcing. They found out that the atmospheric response on sea ice and on SST anomalies resembled the NAO pattern but the amplitude of the response on sea ice was much larger. A decrease in sea ice in the Greenland and Barents Sea and an increase in Labrador Sea ice cover led to a negative phase in the NAO. In agreement with the results of Deser et al. (2000), strong changes in the heat fluxes from ocean to atmosphere occurred due to the anomalies in the ice cover.

Similar investigations have been carried out by Alexander et al. (2004). They used the years with largest and lowest Arctic ice cover from observations during 1979–1999 to force an AGCM and made for each case 50 ensemble runs to evaluate the impact on the atmosphere in the following winter. The local response showed increased ocean-to-atmosphere heat release and decreased SLP where the ice receded and vice versa where sea ice expanded. The large-scale atmospheric response to reduced ice cover east of Greenland resembled the negative phase of the simulated NAO and vice versa.

In this study, the global coupled atmosphere–ocean–sea ice model ECHAM5.0/ MPI-OM is used to investigate the impacts of the variability in the ice export through Fram Strait on climate. A control integration of 500 years of the coupled model provides the possibility of statistical analyses on different timescales. This allows one to present more general statements concerning physical processes than possible with comparatively short-time series of observations and reanalyses. Additionally, the use of a fully coupled atmosphere–ocean–sea ice model enables us to study feedback mechanisms between these climate components. Most previous studies that analysed the impact of Fram Strait ice export were limited to the formation process of GSA's.

Here, we will highlight the affect on both oceanic and atmospheric climate conditions in the Labrador Sea.

2 Model description and climatology

The model used in this study is the Max-Planck-Institute for Meteorology global atmosphere–ocean–sea ice model ECHAM5.0/MPI-OM. It consists of the fifth cycle of the atmosphere model ECHAM (ECmwf HAMburg) and the ocean model MPI-OM (Max-Planck-Institute Ocean Model). The atmosphere model ECHAM5.0 (Roeckner et al. 2003) is run at T42 resolution, which corresponds to a horizontal resolution of about $2.8^\circ \times 2.8^\circ$. It has 19 vertical levels up to 10 hPa. The ocean model MPI-OM (Marsland et al. 2003) is a global version of the Hamburg Ocean Primitive Equation model (HOPE). It includes a Hibler-type dynamic-thermodynamic sea ice model. The grid is based on an Arakawa C-grid and has a resolution of about 2.8° but with an increasing refinement between 30°N and 30° up to 0.5° at the equator from 10°N to 10°S (Fig. 1). The North Pole is shifted towards Greenland (30°W , 80°N) to avoid the grid singularity at the North Pole. The South Pole is located at 30°W , 80°S . Additionally, this has the advantage that the resolution in the Fram Strait and the deep convection areas of Greenland and Labrador Sea is relatively high.

The atmosphere model and the sea ice–ocean model are coupled by the OASIS coupler (Terray et al. 1998). The coupler transfers fluxes of momentum, heat and fresh water from the atmosphere to the ocean and performs the interpolation onto the ocean grid and it transmits sea surface temperature, sea ice thickness and concentration as well as snow thickness from the ocean

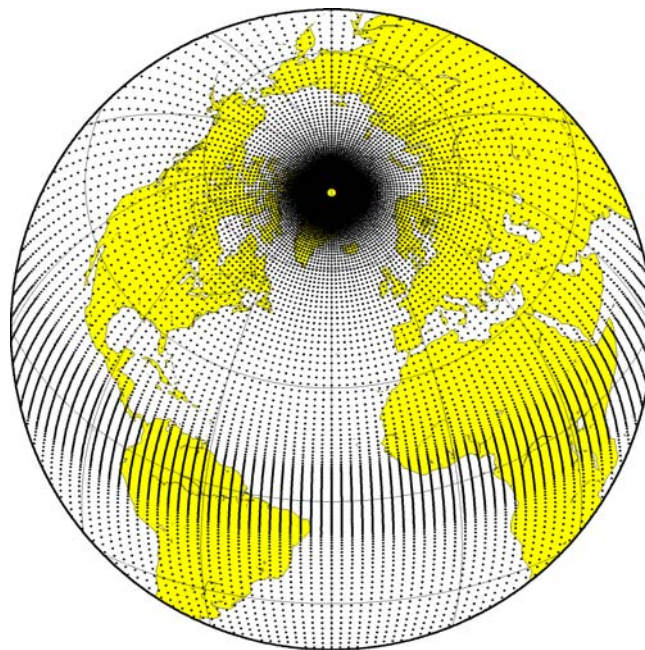


Fig. 1 Grid of the ocean model MPI-OM

to the atmosphere. The climate model includes a river runoff scheme (Hagemann and Dümenil 1998; Hagemann and Dümenil-Gates 2003). The river runoff is transferred together with the precipitation to the ocean. Glacier calving is included in a way that the amount of snow falling on Greenland and Antarctica is instantaneously transferred into the ocean. In the coupled model no flux adjustment is used.

A 500-year control integration from this model has been used in this study. Analyses of multidecadal scale changes in the North Atlantic thermohaline circulation by Latif et al. (2004) and Arctic–North Atlantic interactions by Jungclaus et al. (2005) are based on the same control integration.

Most results are shown for winter-centred annual mean values (August–July). Key components of the climate of the model for the high latitudes of the northern hemisphere are shown in Fig. 2. The SLP agrees well with observations and reanalysis (not shown) in the North Atlantic sector and over most parts of Europe, Asia and North America. However, there are larger differences over the North Pacific. The Aleutian Low is too weak and the Pacific subtropical high is too pronounced. Over the Central Arctic, the pressure is slightly too high, leading to a shift in the transpolar drift stream towards Kara and Barents Sea. The annual mean air temperature shows the typical north south gradient with minimum values of -25°C in Arctic and up to 20°C

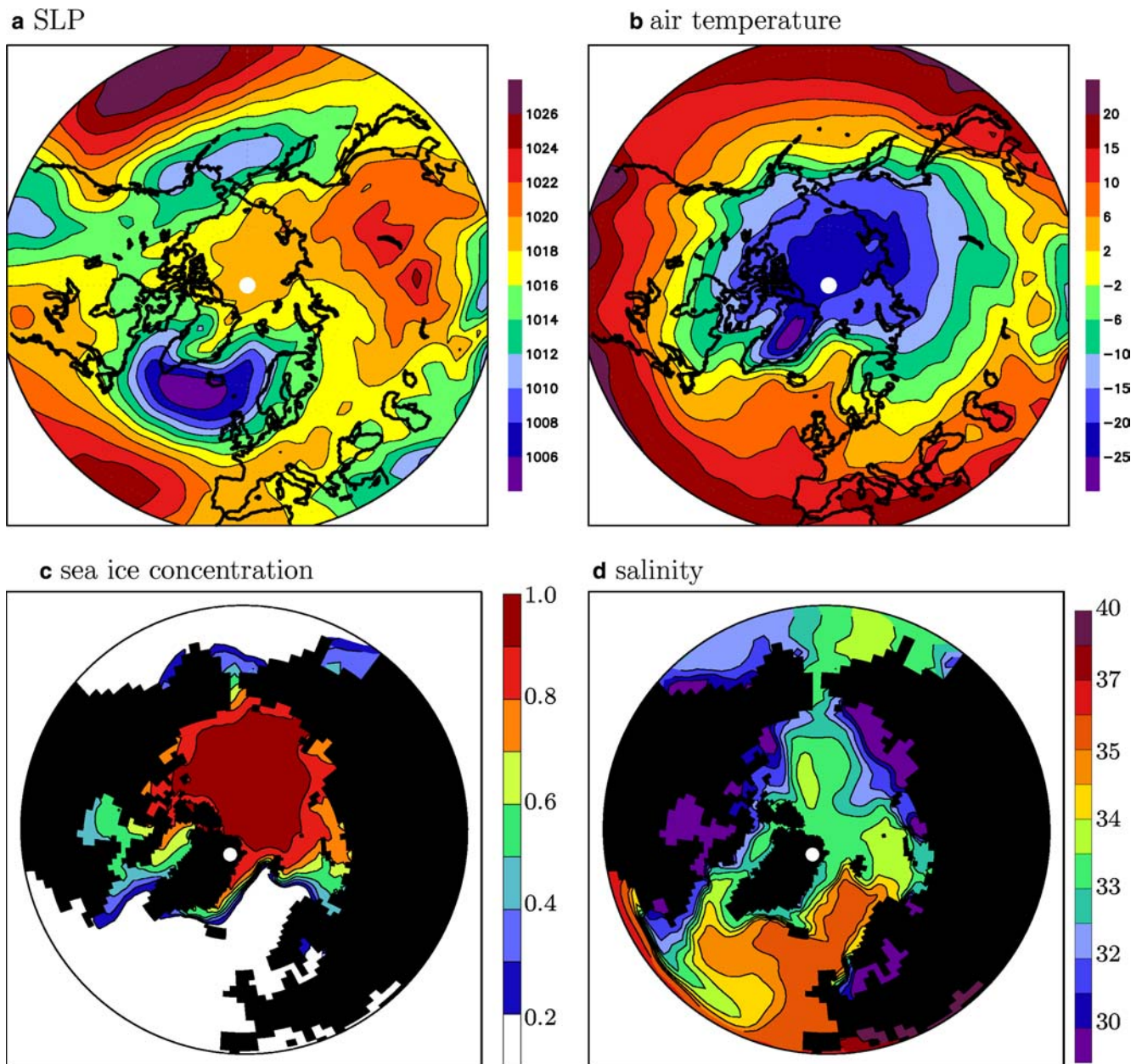


Fig. 2 Model climate: annual mean values for the 500-year control integration **a** SLP in hPa. **b** 2-m air temperature in degrees Celsius. **c** Sea ice concentration in fractions. **d** salinity in psu

south of 30°N. The typical discrepancies from the zonality for example the tongue of warm air in the northeastern North Atlantic and the colder temperatures over Asia are well reproduced. However, the model temperature in general is slightly too cold. Larger discrepancies occur especially over northern and eastern Europe as well as over the northeastern Pacific with about 2 ° and up to 6 ° in parts of the Barents Sea. The large negative bias over the Barents Sea is due to too much ice in this area. The ice slightly extends far south into the Labrador Sea and the Greenland Sea compared to the data of Johannessen et al. (2002). The ice thickness (not shown) is overestimated at the East Siberian Coast, which is a common problem in the other coupled atmosphere–ocean–sea ice models as well (e.g. Goosse et al. 2002; Weatherly et al. 1998). The modelled surface salinity agrees well with the PHC climatology (Polar Science Center Hydrographic Climatology, Steele et al. 2001) in most areas of the North Atlantic and the Nordic Seas. Main discrepancy in this area is a too pronounced low-salinity tongue extending from Newfoundland into the Atlantic. In the Arctic Basin, the model captures well the areas of low salinity at the Siberian and Canadian coast, which is due to the fresh water input of rivers, but in the Central Arctic and the Chukchi Sea the surface salinity is too high.

Figure 3 presents the simulated mean summer and winter climate. The annual SLP pattern in the Arctic is mainly determined by the winter. The SLP gradients in the Arctic are weak during summer. The Siberian High occurs only during wintertime. In contrast, the subtropical highs are more pronounced during summer.

A comparison to NCEP-reanalysis data shows a very good agreement during summer but some larger differences in the North Pacific and the Arctic during winter. The simulated air temperature is characterised by a north–south gradient in the entire year, although it is more pronounced in winter. However, it is slightly colder than in the reanalysis both in summer and winter. The wintertime sea ice extends too far to the south in the Barents and Greenland Seas as well as at the south coast of Alaska in the model compared to observations of Johannessen et al. (2002). During summer too much ice occurs in the Barents Sea and at the Siberian coast. The simulated Arctic surface is in general fresher in summer than in winter because more ice is melted. The salinity gradient across the Greenland Sea is also much more pronounced. The salinity in the model shows a positive bias in the Central Arctic and Chukchi Sea compared to PHC climatology in the entire year.

Altogether the model provides a realistic climate of the high latitudes and has proven to be a useful tool to investigate coupled atmosphere–ocean–sea ice mechanisms.

3 Climate response to the ice export variability

In this chapter, the 500-year control integration is used to analyse the Fram Strait ice export variability and its impact on climate in the northern hemisphere. Figure 4 shows the time evolution of the annual (winter centred) mean ice export through Fram Strait. The mean ice export is with 97,000 m³/s in the upper range of obser-

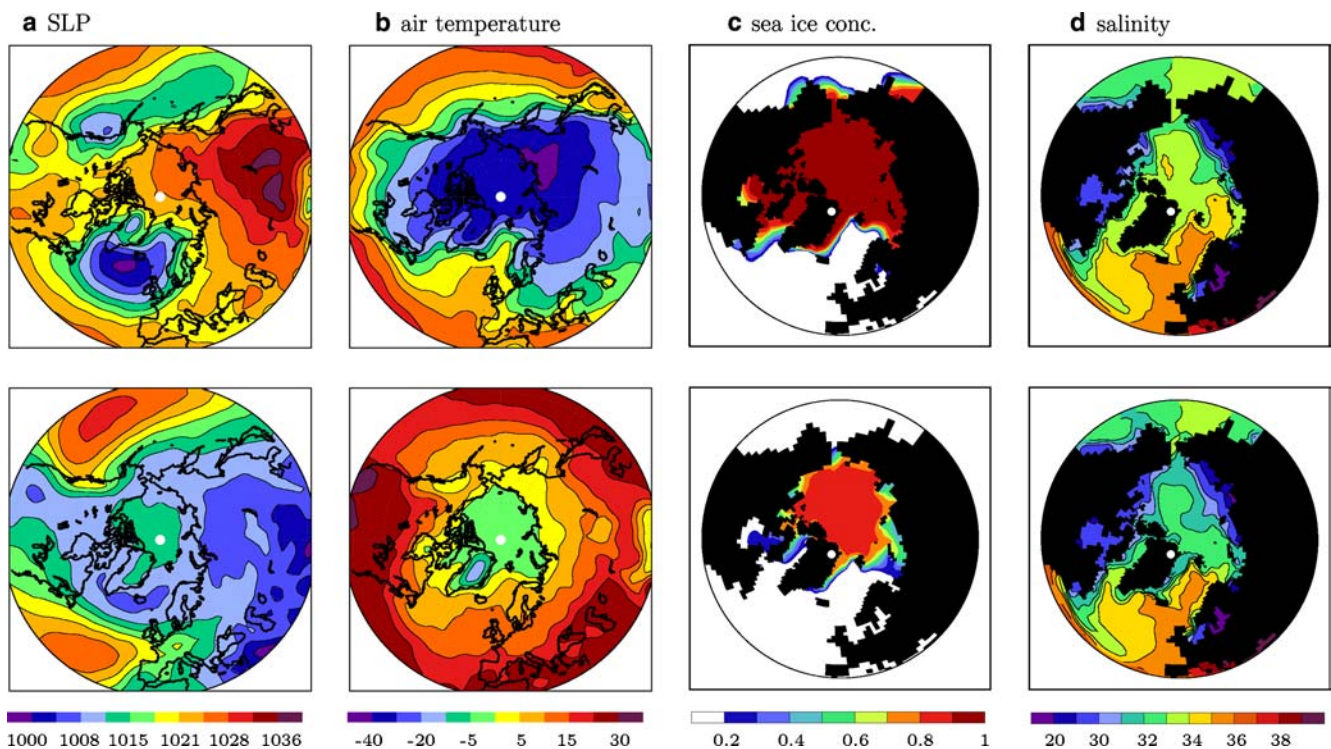


Fig. 3 Same as Fig. 2 but for summer (June, July, August, *top*) and winter (December, January, February, *bottom*) seasons

ventional estimates. Vinje et al. (1998) found for the years 1990–1995 an export of 81,300 m³/s. Aagaard et al. (1989) calculated an ice export of 88,500 m³/s. Estimates of the last 50 years by Vinje et al. (1998) resulted in an export of 92,000 m³/s. In reconstructions of the ice export of Schmith and Hansen (2003) over the last 181 years, the mean reached about 100,000 m³/s. The variability of the ice export in the model is in good agreement with observations as well. In the control integration, annual mean ice exports between 40,000 and 160,000 m³/s are reached. The standard deviation is 20,000 m³/s. A spectral analysis of the modelled ice export (Fig. 5) indicates pronounced peaks at timescales of 3–4, 8–9 and about 15 years.

A peak at roughly 10 years in Fram Strait ice export has been found in several other studies (e.g. Venegas and Mysak 2000; Hilmer and Lemke 2000; Polyakov and Johnson 2000) as well. Furthermore, Venegas and Mysak (2000) and Goosse et al. (2002) showed significant variability in the Arctic ice volume at a timescale of 15–20 years, which might fit to the 15-year peak in this study. Delworth et al. (1997) found a dominant peak at 50 years in the sea surface temperature of Denmark Strait but no high frequency variability. Sea ice dynamics in their model are far from reality and cannot reproduce the interannual variability in the ice export through Fram Strait. Moreover, they show that SLP variations in the Barents and Kara Seas are related to

Fig. 4 Annual mean ice export through Fram Strait

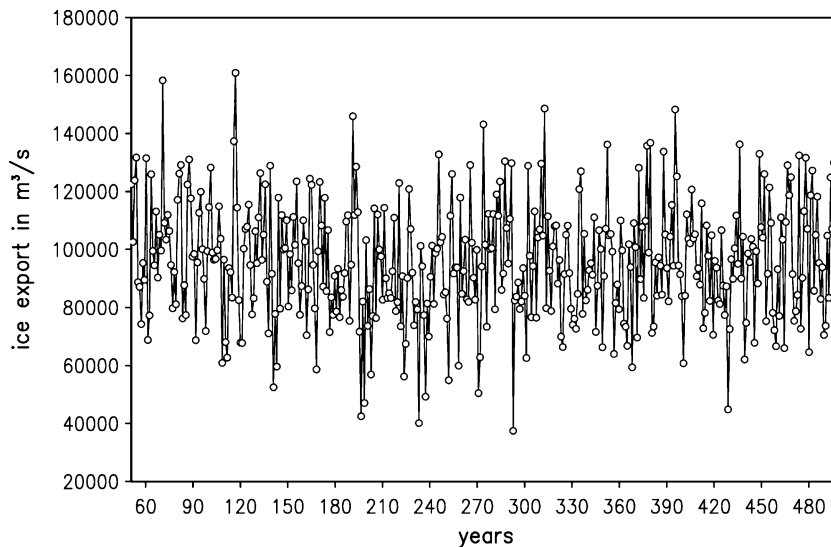
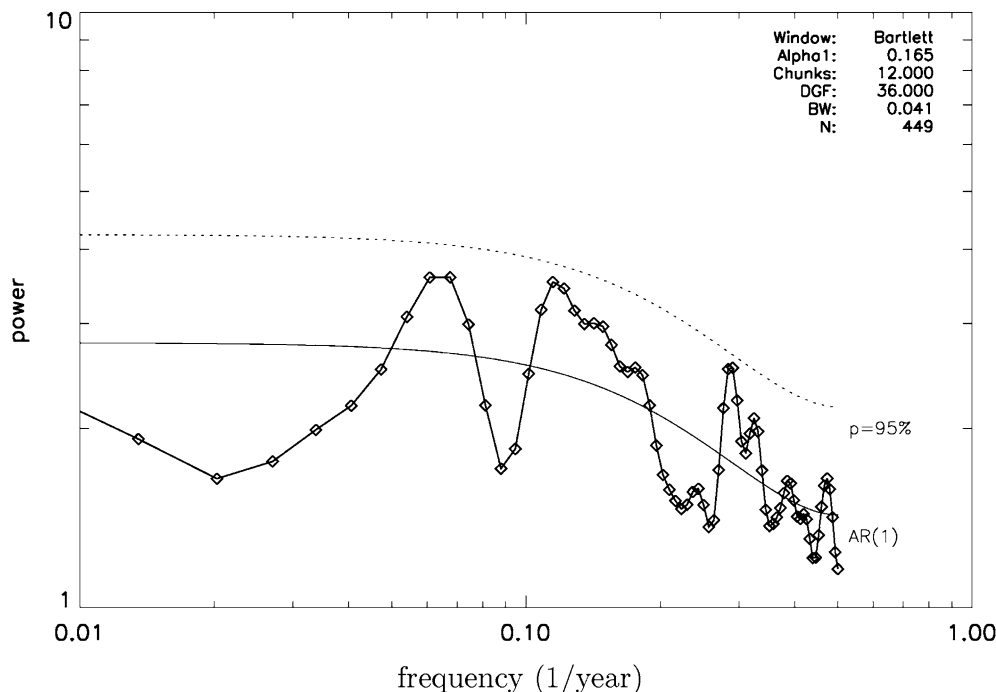


Fig. 5 Spectral analysis of annual mean Fram Strait ice export



SST variations in the Denmark Strait. This agrees well to the correlation pattern between the ice export through Fram Strait and SLP in this study (Fig. 6). The correlation coefficient reaches -0.7 in the area of the Kara Sea (Fig. 6a). Slightly weaker positive correlations are obvious over the Canadian Archipelago. The SLP-gradient across Fram Strait is correlated with the ice export with 0.86 for annual values and explains about three-fourths of the annual mean ice export variability. This is in good agreement with the observational-based estimate of Vinje (2001) who found an explained variance of 80%. Anomalous northerly winds lead to an increase of ice export through Fram Strait, whereas southerly winds reduce it. During periods with northerly winds, both ice velocity and ice thickness in Fram Strait increase. The ice is accumulated by the wind north of Fram Strait and Greenland in this model. Hilmer and Jung (2000) and Kwok and Rothrock (1999) found a positive correlation between the ice export and the North Atlantic Oscillation since 1978 (NAO, Hurrell 1995; Hurrell and van Loon 1997). Before 1978 and in model simulations (Jung and Hilmer 2001), no significant correlation could be found. In our model, the NAO has neither direct influence on the ice export nor on the SLP gradient across Fram Strait. Lag correlations and the analysis of 30-year periods gave no significant results either.

Ice volume anomalies have a substantial impact as well. Figure 7 shows a lag regression of ice thickness anomalies with the ice export through Fram Strait. Five years before high ice exports, positive ice thickness anomalies are formed at the coasts of Chukchi and East Siberian Sea (Fig. 7a)). In agreement with results of Tremblay and Mysak (1998), these anomalies are caused by a convergent ice transport due to an anomalous wind field associated with a negative ice export through Fram Strait. In the next 2 years, the positive ice thickness anomaly slowly propagates clockwise along the Siberian coast (Fig. 7b)) and crosses the Arctic to reach Fram Strait leading the ice export by 1 year (Fig. 7c)). High

ice exports themselves are associated with large anomalous ice transports all over the Arctic towards Fram Strait (Fig. 6b)) due to the anomalous atmospheric forcing described above (Fig. 6a)). As a consequence, a negative ice thickness anomaly occurs at the Siberian coast. It propagates across the Arctic to Fram Strait in the next years, which leads to a decreased ice export (Fig. 7e, f)) 4 years later. A further year later the ice export through Fram Strait is still reduced and ice thickness at the Siberian coast is again increased. The entire cycle takes about 9 years and matches the peak in the power spectrum of the ice export at the same time-scale (Fig. 5).

The impact of anomalous ice exports on the climate of the following years is examined by using composite analyses for different climate parameters. The cases of high and low ice export events through Fram Strait are investigated separately. We define large ice exports as positive anomalies of more than one standard deviation and vice versa.

The ice, exported anomalously through Fram Strait, propagates southwards in the East Greenland Current and melts. A part of the fresh water remains in the Greenland Sea but the predominant amount flows into the Labrador Sea. This fresh water anomaly forms a large negative salinity anomaly in the Labrador Sea 1–2 years later (Fig. 8, left). The model is able to reproduce the formation of GSA's in the Labrador Sea shown by Häkkinen (1999) and Haak et al. (2003). Apparently, the ice export through Fram Strait is the main factor for these anomalies. Table 1 shows that salinity is decreased within 1–3 years after high ice exports in 35 of the 39 cases. Nineteen of these events lead to major negative salinity anomalies in the Labrador Sea. In the four cases where salinity increases after high ice export events, the fresh water does not reach the Labrador Sea due to strong anomalous winds. They deflect the ice to the east, south of Fram Strait or at the southern tip of Greenland. The anomalous fresh water inflows into the Labrador

Fig. 6 **a** Correlation pattern between annual mean ice export through Fram Strait and sea level pressure. **b** Regression pattern between Fram Strait ice export and sea ice transport in the Arctic in $10^{-3} \text{ m}^2/\text{s}$ per standard deviation ice export

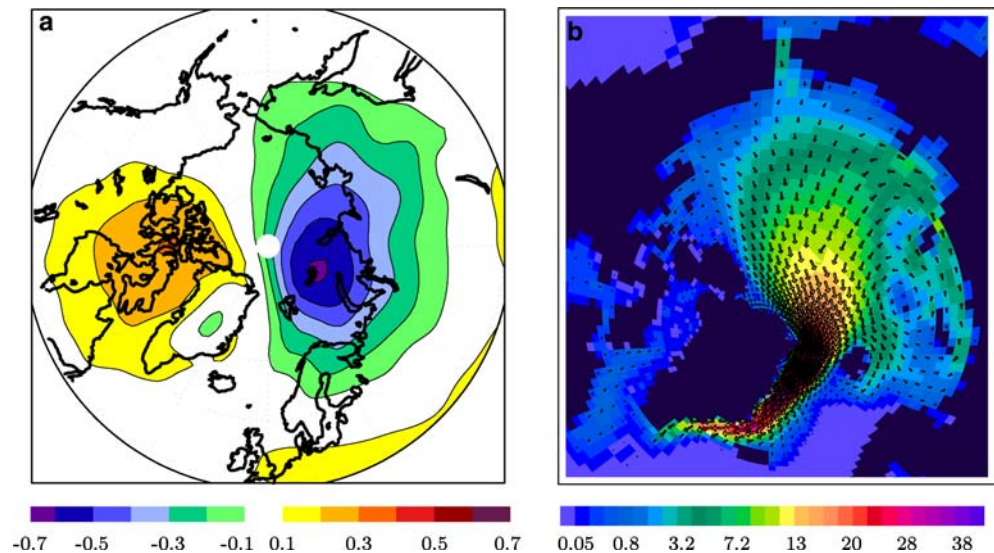
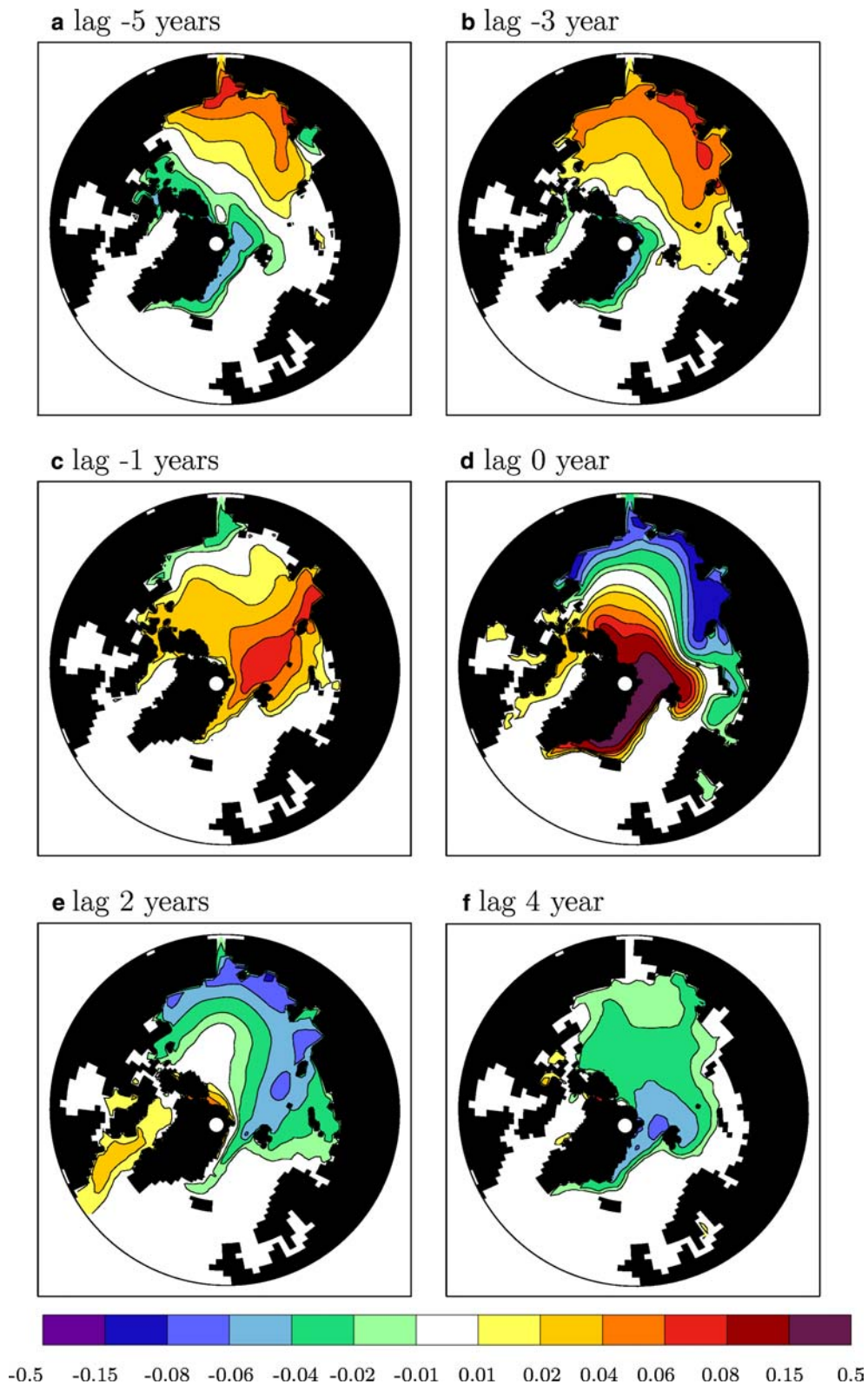


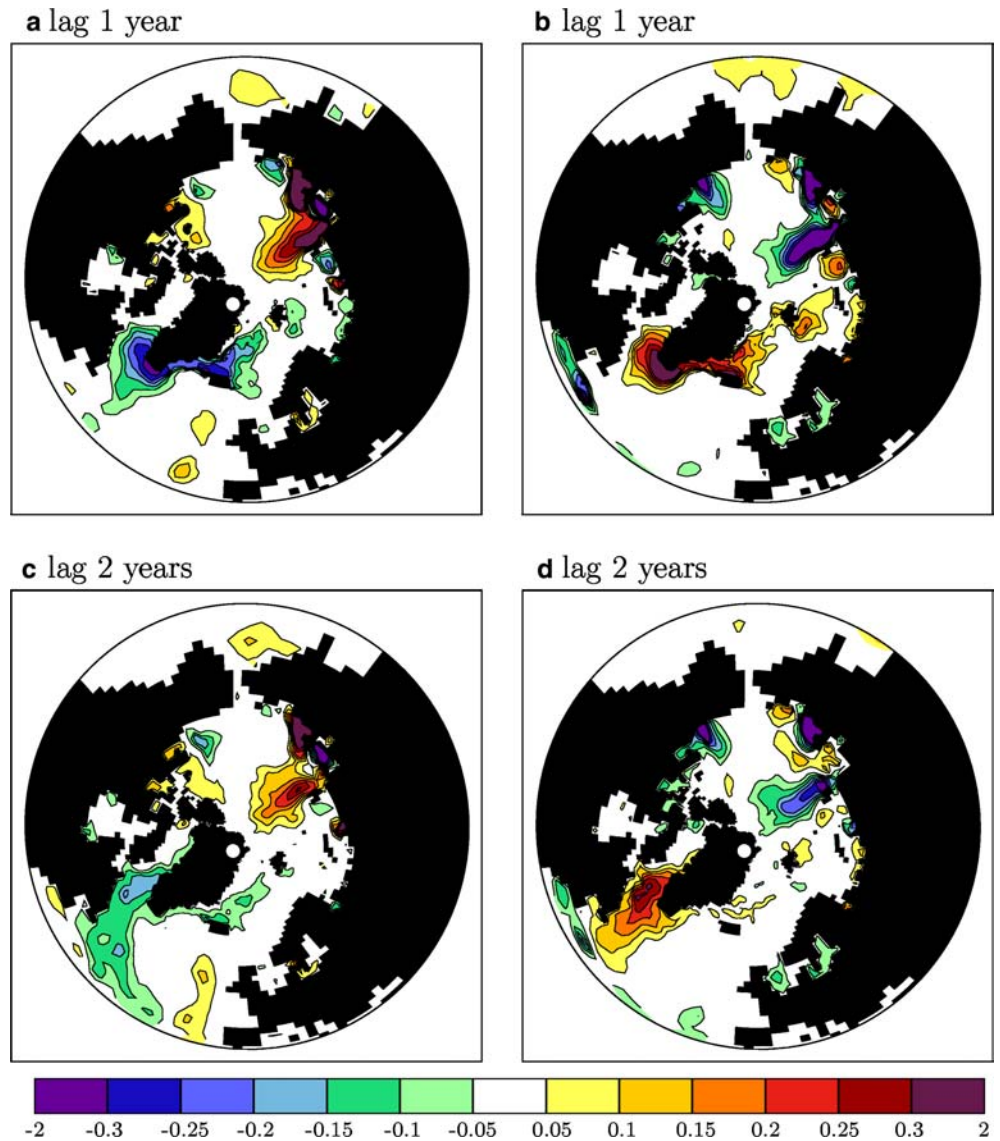
Fig. 7 Regression coefficient between annual mean values of the ice export through Fram Strait and ice thickness anomalies **a** Ice export lags 5 years. **b** Ice export lags 3 years. **c** Ice export lags 1 year. **d** lag 0. **e** Ice export leads 2 years. **f** Ice export leads 4 years



Sea through the Davis Strait, the Hudson Bay, the southern boundary and from precipitation are much smaller than the anomalous inflow by the East Greenland Current. Other studies such as Goosse et al. (1997) estimated the fresh water flux through the Canadian

Archipelago and local processes (Houghton and Visbeck 2002) to be more important for the water properties in the Labrador Sea than assumed in our model. It should be noted that the model resolution is not sufficient to resolve the Canadian Archipelago properly. Therefore,

Fig. 8 Composite analysis for annual mean 10 m salinity anomalies in psu 1 and 2 years after high (*left*) and low (*right*) ice exports through Fram Strait



the ice export, through it, is probably underestimated. Nevertheless, about 20% of large negative salinity anomalies cannot be explained by prior export anomalies through Fram Strait. They occur due to fresh water inflow through the other three boundaries of the Labrador Sea or due to fresh water inflow through the eastern boundary, which is not associated with previous large ice exports through Fram Strait. The local mixing

of surface waters with deeper layer waters, which is driven by atmospheric forcing (e.g. high or low NAO-index), plays a role as well. Table 2 summarises that low ice exports, through Fram Strait, that lead to positive salinity changes in the Labrador Sea.

The fresh water input in the Labrador Sea after large ice export events stabilises the local stratification of the ocean. Deep convection is decreased or even totally suppressed 1–2 years after high ice exports. This is evidenced by a considerable reduction in the late winter/early spring (February, March, April) mixed layer depth up to 700 m in the Labrador Sea. Compared to the mean convection depth of 1,500 m, mixed layer depth is reduced by almost half (Fig. 9, left). In the Greenland Sea, it is decreased by 200 m. This mainly reflects a change in the position of deep convection. After low ice exports, there is a deepening in the mixed layer depth and thus an increased convection is obvious in the Labrador Sea. On an interannual timescale, no significant correlation between the salinity in the Labrador Sea and the

Table 1 Distribution of the maximum year-to-year decrease in 10 m salinity (ΔS) within 3 years after positive Fram Strait ice export events. Thirty-nine years with ice export anomalies exceeding 1.5 standard deviations are used. The salinity is averaged over the central Labrador Sea and the ΔS are given in standard deviations

	$\Delta S < -1$	$-1 < \Delta S < -0.5$	$-0.5 < \Delta S < 0$	$\Delta S > 0$
Number years	19	8	8	4
%	48.7	20.5	20.5	10.3

Table 2 Same as Table 1 but positive salinity changes using 23 years with negative ice export anomalies exceeding 1.5 standard deviations

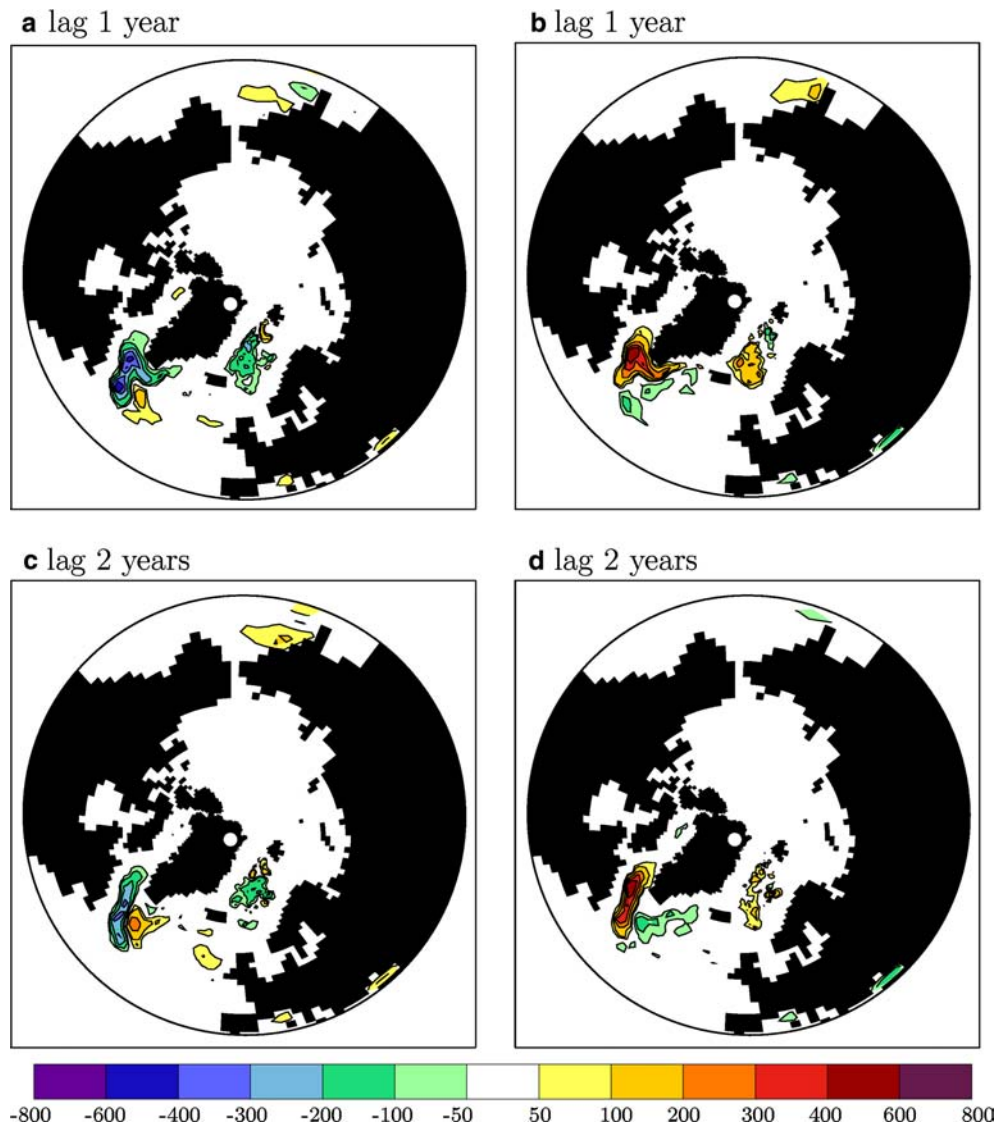
	$\Delta S > 1$	$0.5 < \Delta S < 1$	$0 < \Delta S < 0.5$	$\Delta S < 0$
Number years	13	6	1	3
%	56.5	26.1	4.3	13.1

meridional overturning could be found in our model. This agrees well with results of Power et al. (1994) but is contrary to findings of Häkkinen (1999). However, for longer timescales the surface salinity of the Labrador Sea and the meridional overturning are highly positively correlated. It takes several years to consume the reservoir of deep water in the Labrador Sea, which is formed during such 1 year with strong deep convection. Thus, a single year with large or without deep convection has no significant influence on the meridional overturning. If salinity anomalies could persist for more than a few

years in the Labrador Sea, there would be a large influence on the entire thermohaline circulation (Jungclauss et al. 2004, in press). This might happen after large ice export anomalies that were shown by Mikolajewicz et al. (submitted) in model simulations with a regional coupled atmosphere–ocean–sea ice model.

The anomalous sea ice export through Fram Strait affects sea ice concentration in the Greenland (especially in the first year after the anomalies, not shown) and the Labrador Sea 1–2 years later (Fig. 7e)). The increase of sea ice in the Greenland Sea after high ice export events is due to the direct effect of enhanced ice transport into the Greenland Sea (Walsh and Chapman 1990; Wang and Ikeda 2000). In addition, increased ice export is associated with the anomalous advection of cold air from the north into the Greenland Sea. This leads to an intensified sea ice formation in winter and less melting in summer. Sea ice cover increases in the Labrador Sea, because anomalous cold and fresh water is transported into the Labrador Sea after large ice export events. In

Fig. 9 Composite analysis for late winter/early spring (February, March, April) mixed layer depth anomalies in metres 1 and 2 years after high (*left*) and low (*right*) ice exports through Fram Strait



the first year, sea ice concentration is increased by 10% both in Labrador and Greenland Sea (not shown). One year later, the ice anomaly is much more pronounced in the Labrador Sea than in the Greenland Sea because convection in the Labrador Sea is still weak. Therefore, surface waters are still colder and fresher than usual. Deser et al. (2002) found a good correlation between salinity in the West Greenland Current and sea ice in the Davis Strait, which is in good agreement to our results. They determined three periods with especially large and long-lasting sea ice anomalies from an EOF analysis of sea ice concentration data from 1953–1997: 1972/1973, 1983/1984 and 1990/1991. Additional model simulations by Deser et al. (2002) indicate that these anomalies were accompanied by a northwesterly atmospheric flow in the Davis Strait/Labrador Sea. However, before all the three sea ice events, high ice exports through Fram Strait had occurred (Haak et al. 2003). Similar investigations for annual values of sea ice concentration from our control run show that the NAO is correlated with the sea ice concentration in Davis Strait with 0.38. The ice export through Fram Strait has about the same correlation coefficients with the sea ice concentration for lags of 1–2 years. In the next section, we will show that the northwesterly wind anomalies in the Labrador Sea, as found by Deser et al. (2002), are formed 2 years after large ice exports. They are thus part of the entire process.

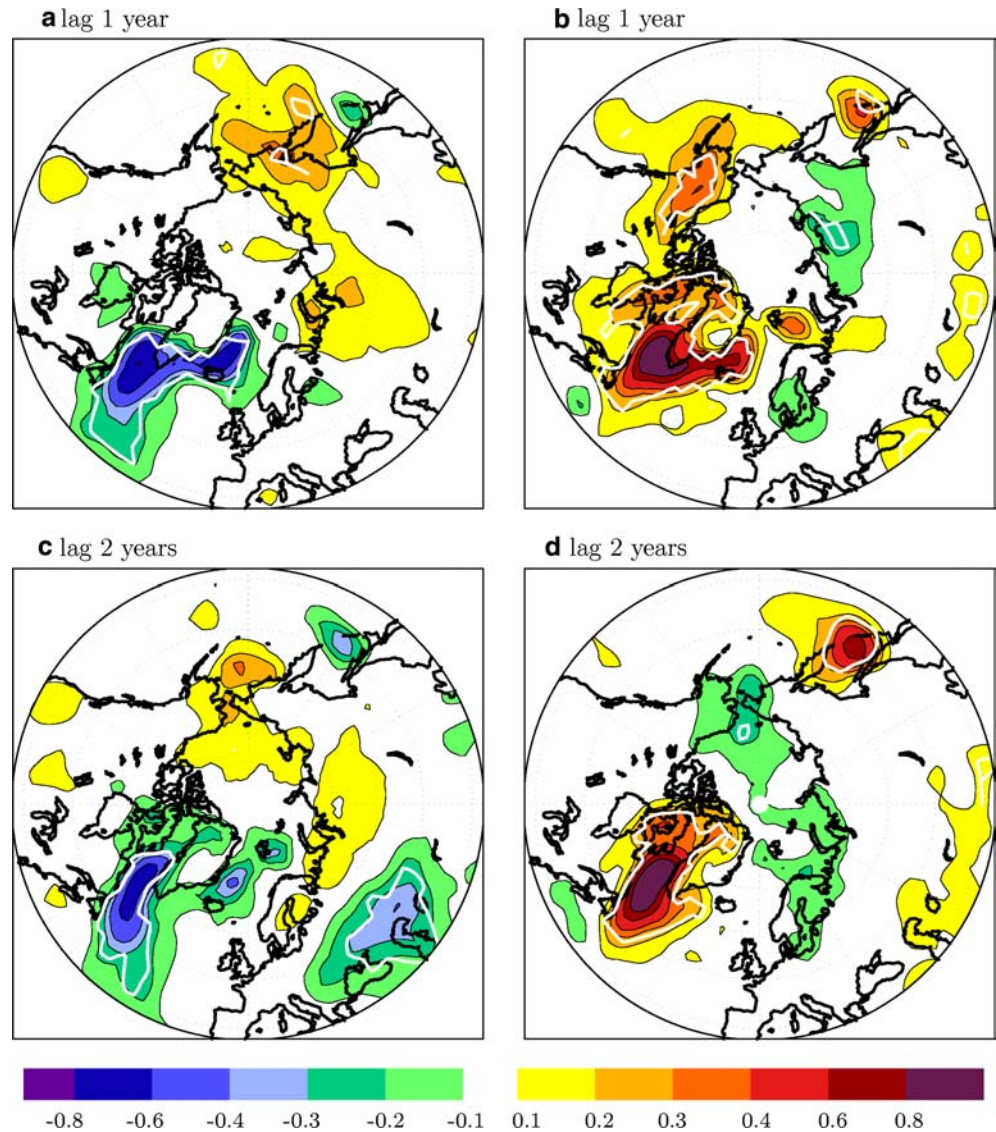
Both the decrease in convection and the increase in the ice concentration in our model are responsible for a reduced ocean heat release to the atmosphere in the Greenland and Labrador Seas. Over the North Atlantic, the ocean heat release is increased after large ice exports. The northern North Pacific also seems to be affected. Positive anomalies in the ocean heat release are simulated in the Bering Strait and negative anomalies north of Japan. These anomalies in the heat flux are mainly due to the anomalous advection of cold or warm air masses, except for those in the Labrador and Greenland Seas. Again, the response is symmetric and low ice exports through Fram Strait lead to a decrease in the ice concentration of similar magnitude. The anomalies in the ocean heat release have consequently the opposite sign. These heat flux variations have a direct impact on atmospheric climate conditions. Figure 10 shows the resulting 2-m air temperature anomalies 1–2 years after large and low ice exports. The reduced ocean heat release to the atmosphere (after large ice export) causes much colder temperatures in the Labrador and Greenland Seas. Anomalies of up to 1 K for annual values and 2 K for winter means (December, January, February, not shown) are reached in the Labrador Sea. They are highly significant using a two-tailed *t* test. Significant anomalies are also obvious in the area of the Caspian Sea and over smaller parts of the North Pacific. They are mainly due to changes in the large scale atmospheric circulation (Fig. 11). The largest SLP anomalies can be seen over the North Atlantic and the European Arctic. Two years after large ice exports, a dipole occurs with positive SLP anomalies up to 0.6 hPa over the North

Atlantic and negative anomalies up to -0.6 hPa over the Nordic Seas. The pattern resembles the positive NAO-index pattern and vice versa, both 1–2 years after low ice exports. SLP anomalies are significant only locally at the 95% level but larger areas reach the 90% significance level. We suggest the following mechanism: Large ice export leads to an increase in the ice area in the Greenland and Labrador Sea and an enhanced north–south temperature gradient over the North Atlantic. Atmospheric heat flux to the north has to be increased to reduce this temperature gradient. This is done by enhanced synoptic activity. Murray and Simmonds (1995) investigated the effect of a progressive removal of sea ice in the Arctic on the atmospheric circulation and found a weakening of the Iceland Low and a decrease in pressure over the eastern North Atlantic and southern Europe.

To compare the atmospheric response in the model with NCEP/NCAR-reanalysis (Kalnay et al. 1995), the Fram Strait ice export from the uncoupled ocean model MPI-OM forced with NCEP-reanalysis data has been used (as done in Haak et al. (2003)). The composite analyses for annual mean 2-m air temperature and SLP anomalies in the reanalysis are shown in Fig. 12. We have to take into account that only five events with large ice export through Fram Strait occurred during the 50 years of NCEP reanalysis. Therefore, statistics are poor and it is difficult to make general statements. Nevertheless, the composite analysis of the air temperature shows negative anomalies in the Labrador Sea of similar magnitude as in the coupled model after large ice exports. The SLP-pattern indicates the main features of the modelled results. Furthermore, there is a obvious positive NAO-index in the reanalysis 2 years after large ice exports.

It has been shown above that air temperature variability in the Labrador Sea is strongly dependent on the variability of ice export through Fram Strait and the associated salinity and heat flux anomalies in the Labrador Sea. The correlation of annual mean air temperature and surface salinity (both variables are averaged over a box in the central Labrador Sea ($54\text{--}60^\circ\text{N}$, $48\text{--}56^\circ\text{W}$)) is 0.78. This means that slightly more than 60% of the temperature variability can be explained by surface salinity in the Labrador Sea. The advection of air masses also greatly affects temperature. The NAO-index is a good indicator for this: in years with positive NAO-index, anomalous cold air is advected from the Arctic to the Labrador Sea and in the negative NAO-case warm air is advected from the Atlantic. The correlation coefficient between air temperature in the Labrador Sea and the NAO-index is -0.48 . Since no significant correlation between surface salinity in the Labrador Sea and NAO-index is found ($r=0.02$), it seems that there are two independent processes operating. Therefore, we compute an index consisting of the difference of the normalised salinity and the normalised NAO-index. The maximum of correlation between this index and air temperature in the Labrador Sea is reached when salinity is weighted with 1.3 and the NAO-index with 0.7. Then the corre-

Fig. 10 Composite analysis for annual mean 2-m air temperature anomalies in Kelvin 1 and 2 years after high (*left*) and low (*right*) ice exports through Fram Strait



lation coefficient amounts to 0.9 and about 80% of the total variance in the temperature is thus explained.

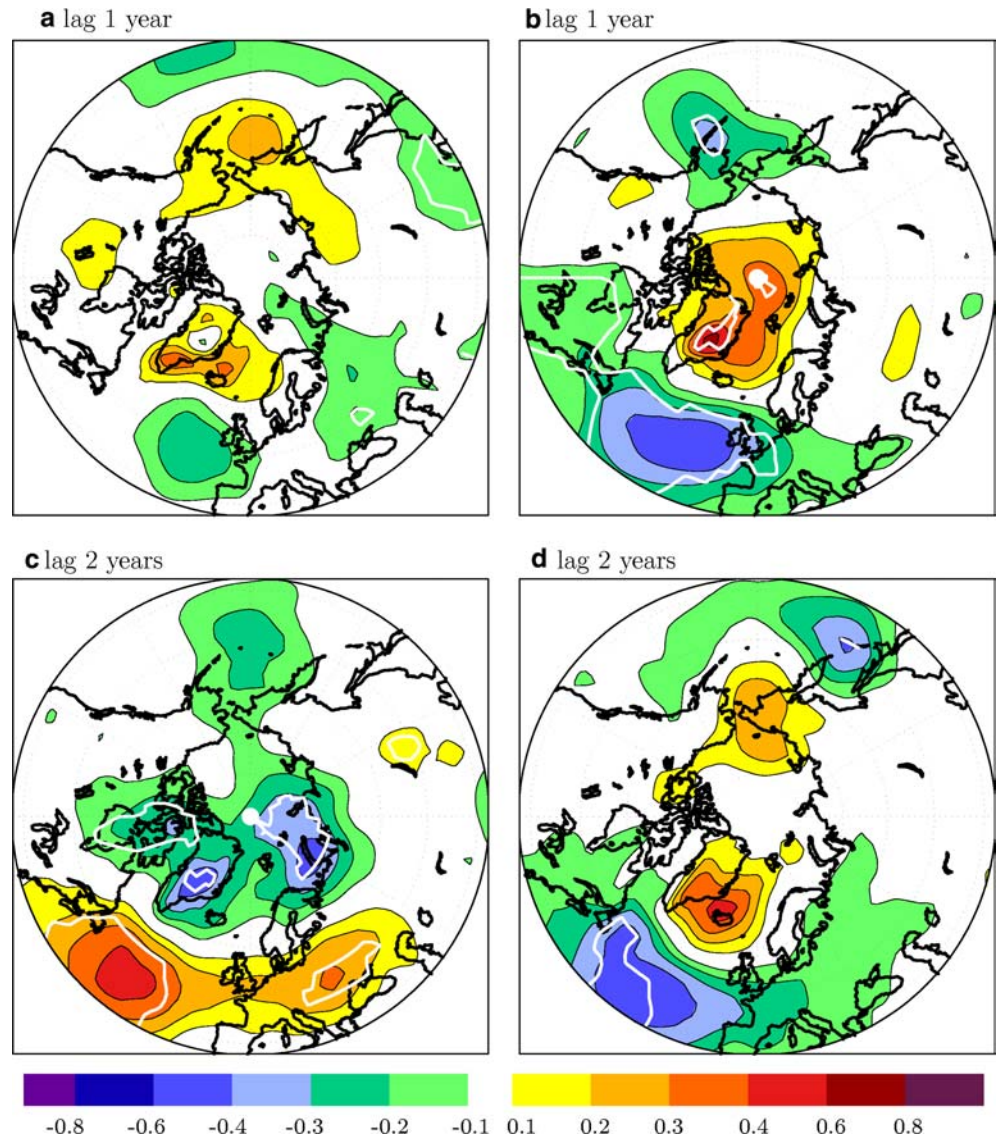
4 Sensitivity studies

The large influence of anomalous ice exports through Fram Strait on climate in the Labrador Sea of the following years has been shown above. In order to analyse the isolated impact of the ice/fresh water signal, associated with high ice exports through Fram Strait, the effect of large ice exports is prescribed in model simulations. Additionally, it should be proved that the anomalies in the Labrador Sea after anomalous ice exports are to a large extent independent from certain starting conditions in the atmosphere and the ocean. As initial conditions, 20 different years from the control run, with close to normal winter ice exports through Fram Strait, are used. Each run is started at the end of April with a single input of an ice volume anomaly of 3,000 km³ into

the East Greenland Current, south of Fram Strait. The amount of ice has been chosen according to the ice export through Fram Strait before the GSA in 1970/71. Each simulation is run for 5 years.

Figure 13 shows seasonal mean (DJF, MAM, JJA, SON) surface (10 m) salinity and 2-m air temperature anomalies in the central Labrador Sea in the first 4 years after the prescribed ice export anomaly. Temperature and salinity are averaged over an area bounded by 54–60°N, 48–56°W. The anomalies describe the mean differences between the seasonal values of the 20 experiment runs and the 500-year control run and the same for the associated 20 control runs. The standard deviations were calculated from the 500-year control integration as quantity for the magnitude of the anomalies. The added ice melts while propagating southwards and reaches the Labrador Sea after approximately 1 year. Surface salinity (Fig. 13, top) is reduced and reaches its minimum one and a half years after the export event. The salinity anomaly has a magnitude of more than two

Fig. 11 Composite analysis for annual mean SLP anomalies in hPa 1 and 2 years after high (left) and low (right) ice exports through Fram Strait

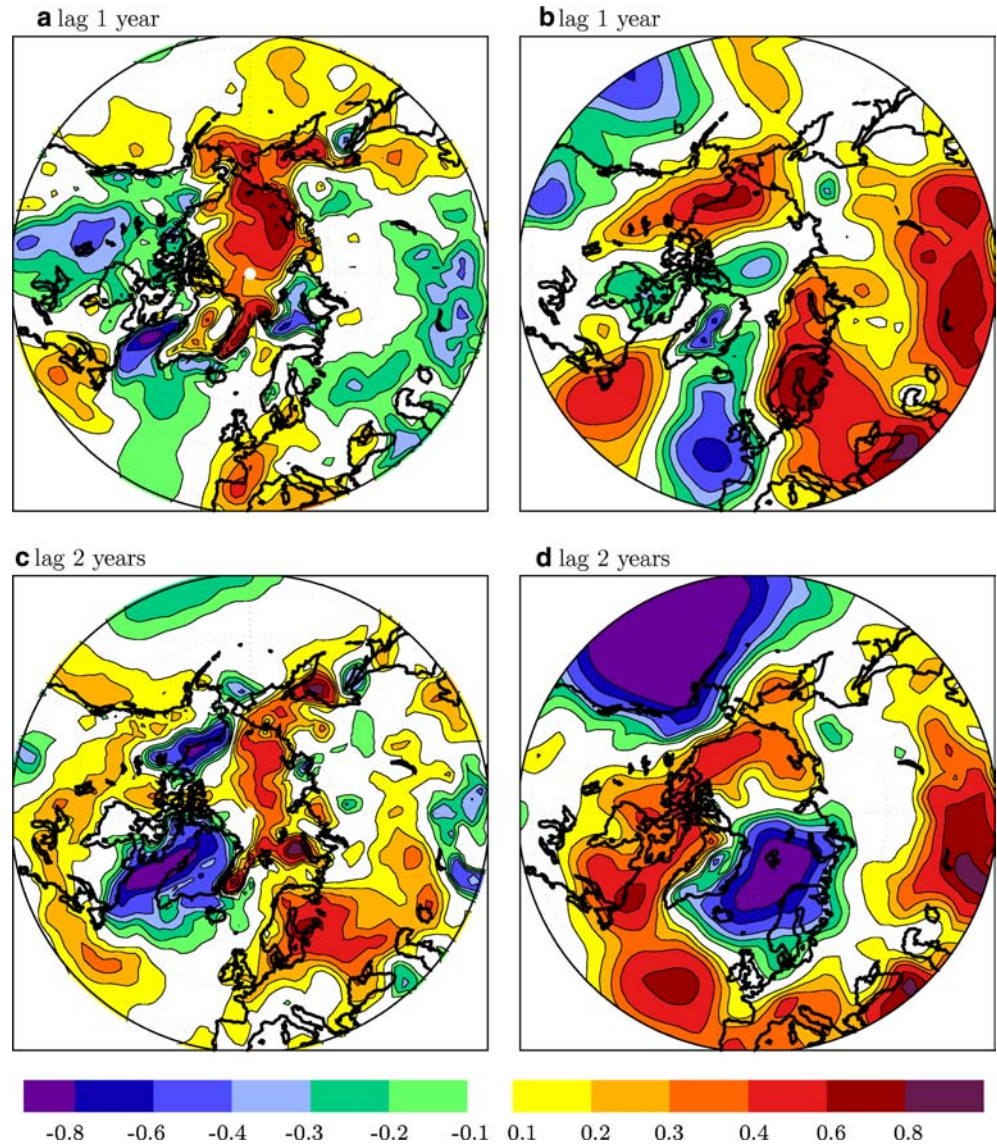


standard deviations. A two-tailed t test shows that it is statistically highly significant. It takes 4 years until the salinity recovers. Observations of the GSA in the early 1970s from the Ocean Weather Ship Bravo show similar surface salinity anomalies in the central Labrador Sea (e.g. Dickson et al. 1988; Lazier 1995). The observations confirm that it took about 4–5 years to reinstall normal conditions. But the propagation time of the fresh water anomaly from the Fram Strait to the Labrador Sea was about 1 year longer than typical in our model simulations. In idealised simulations of the GSA in a coupled ocean–sea ice model by Häkkinen (1999), surface salinity anomalies reached -1 psu in the Labrador Sea in the second and third year after ice export. This led to SST anomalies in the same area of up to -2.5 K.

In contrast to the salinity, the modelled temperature anomalies (Fig. 13, bottom) exhibits a pronounced seasonal cycle. The largest values occur in winter with a maximum of four Kelvin in the first winter. Nevertheless, the temperature anomalies are highly significant in

spring and summer as well. During autumn, anomalies are smallest and the significance is slightly weaker. Again, it takes 4 years to reinstall normal temperature conditions in the Labrador Sea. The spatial distribution of the air temperature anomalies 1–3 years after the simulated ice export shows by far the largest anomalies in the area of the Labrador Sea (Fig. 14). However, significant anomalies also occur in some other regions. Positive anomalies extend from the Ural Mountains to the Ochotsk Sea after 1 and 3 years. In contrast to the first and third year, there is a weaker negative ice anomaly at the East Siberian coast (not shown) and reduced advection of warm air to Siberia 2 years after the ice export. This might explain the lack of positive temperature anomaly in year two, but its existence in the years one and three. Furthermore, positive anomalies although not statistically significant at the 95% level are apparent over parts of Europe after 2 and 3 years. A temperature decrease occurs over the Gulf of Alaska and north of the Caspian and Black Seas after 1 year and

Fig. 12 Composite analysis for annual mean NCEP 2-m air temperature (**a** in Kelvin) and SLP (**b** in hPa) anomalies 1 (*top*) and 2 years (*bottom*) after high ice exports through Fram Strait



over the Bering Sea and the Canadian Archipelago after 2 and 3 years. These temperature anomalies are mainly caused by changes in the wind field, except for those in the Labrador Sea. The associated variations in the SLP-field are shown in Fig. 15. There are only small areas with significant changes 1 year after the ice export. Lower SLP than usual can be seen at the Siberian coast and east of Japan while SLP is increased over the Bering Sea. In the years lagged by 2 and 3 years, a positive pressure anomaly extends from the Labrador Sea across the Atlantic to the southwest of Europe. SLP is reduced further north over Scandinavia and the Nordic Seas. Therefore, the SLP pattern is similar to the positive phase of the NAO. These results correspond to those obtained both from the control run and from the run with NCEP-reanalysis. Two and three years after the prescribed ice export, a pressure gradient across the Arctic with low pressure over the Nordic Seas and anomalous high pressure over the Chukchi Sea is

formed. This pressure gradient amplifies the transpolar drift stream, which implies that more ice is transported from the Siberian coast across the Arctic towards Greenland and Fram Strait. In the model experiments this leads to an increased ice export through Fram Strait (Fig. 16). The anomaly amounts to 0.5 standard deviation and is significant at the 90% significance level. This positive feedback from the inserted ice on the ice export in this model experiment matches the 3–4-year peak in the spectral analysis of the ice export in the control run. However, the results from the control integration show negative ice thickness anomalies 3–4 years after large ice export events as part of the 9-year mode. One has to consider that a negative ice anomaly at the Siberian coast is not explicitly described in the experiment while such an anomaly occurs during high ice exports in the control run. Nevertheless, analysis of the ice export in the control run with a wavelet analysis (not shown) indicates that the 3-year cycle only shows up when the

Fig. 13 Seasonal mean 10 m salinity (*top*) and 20-m air temperature (*bottom*) anomalies in the Labrador Sea. Means of the 20 experiment runs (*blue*) and the associated control runs (*black*). The *dashed black line* indicates -1 SD of the 500 years control run. A blue cycle (*filled blue cycle*) indicates significance on the 95% (99%) level. The time axis starts with the summer season (JJA) in the year with the inserted ice anomaly

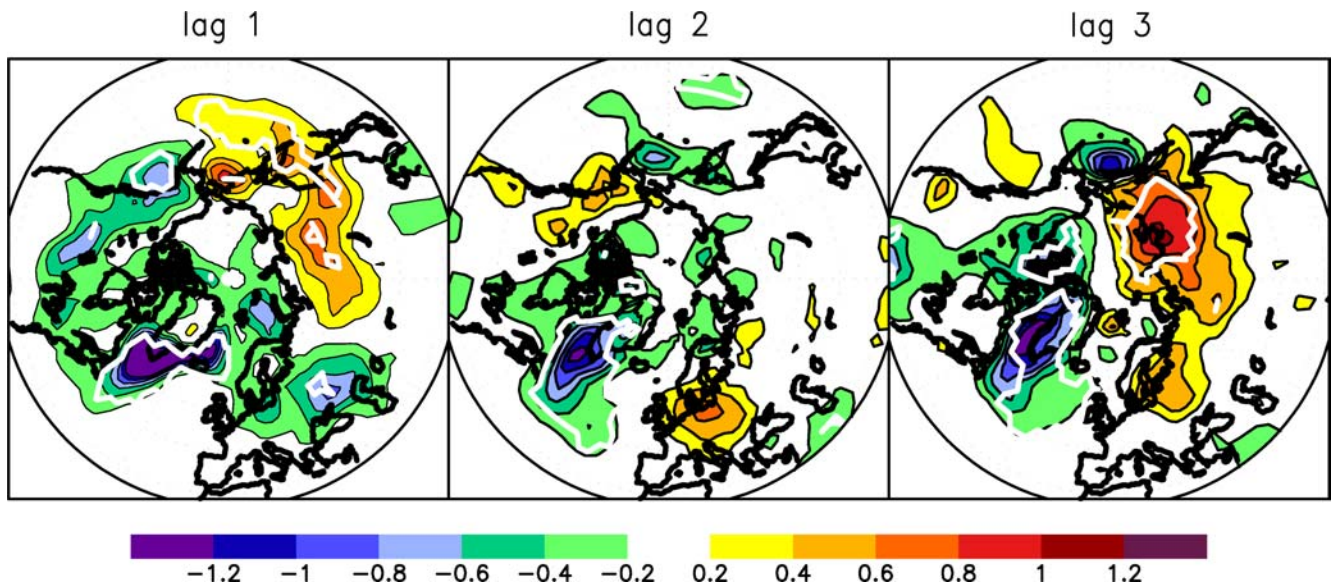
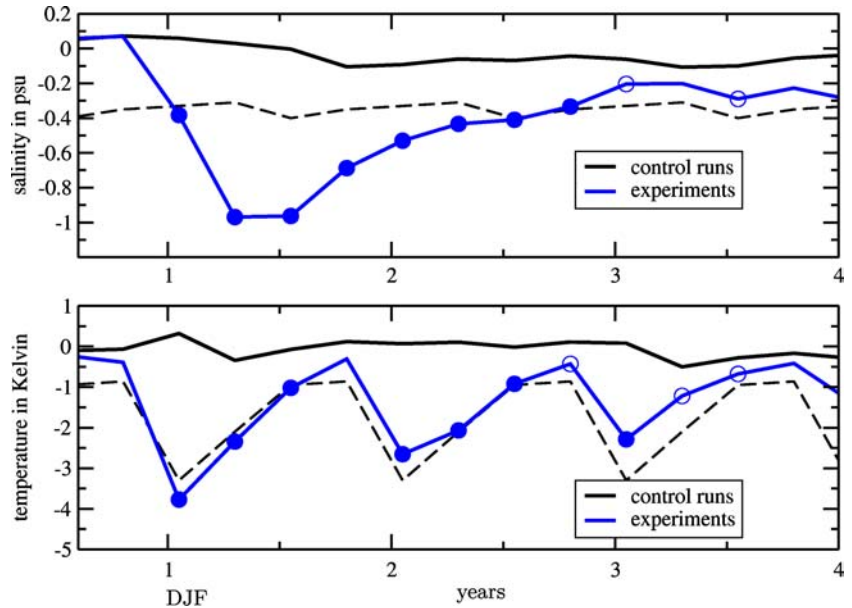


Fig. 14 Annual mean 2-m air temperature anomalies 1–3 years after the ice export. Mean of the 20 runs. The *white line* indicates the level of 95% significance

9-year oscillation is not active. Otherwise the 3–4-year mode is suppressed by the 9-year mode and thus not apparent.

5 Predictability of Labrador Sea climate

In the sensitivity studies above it has been demonstrated that the isolated effect of the ice/fresh water signal after extreme ice exports through Fram Strait accounts for a considerable fraction of climate variability in the Labrador Sea. In this chapter, we will explore the potential use of Fram Strait sea ice export as predictor for Lab-

rador Sea climate after 1 and 2 years. The predictability is analysed for annual mean values of 10 m salinity and 2 m air temperature.

Table 3 shows the statistical probability for salinity anomalies 1 and 2 years after 68 large (more than one standard deviation) positive and 70 negative ice export anomalies in the 500-year control integration. The cases of positive salinity anomalies, anomalies larger than one standard deviation, negative anomalies and anomalies exceeding -1 SD are analysed. The mean distribution for all years of the control run is given for comparison. The probability for a negative salinity anomaly in the central Labrador Sea after large ice

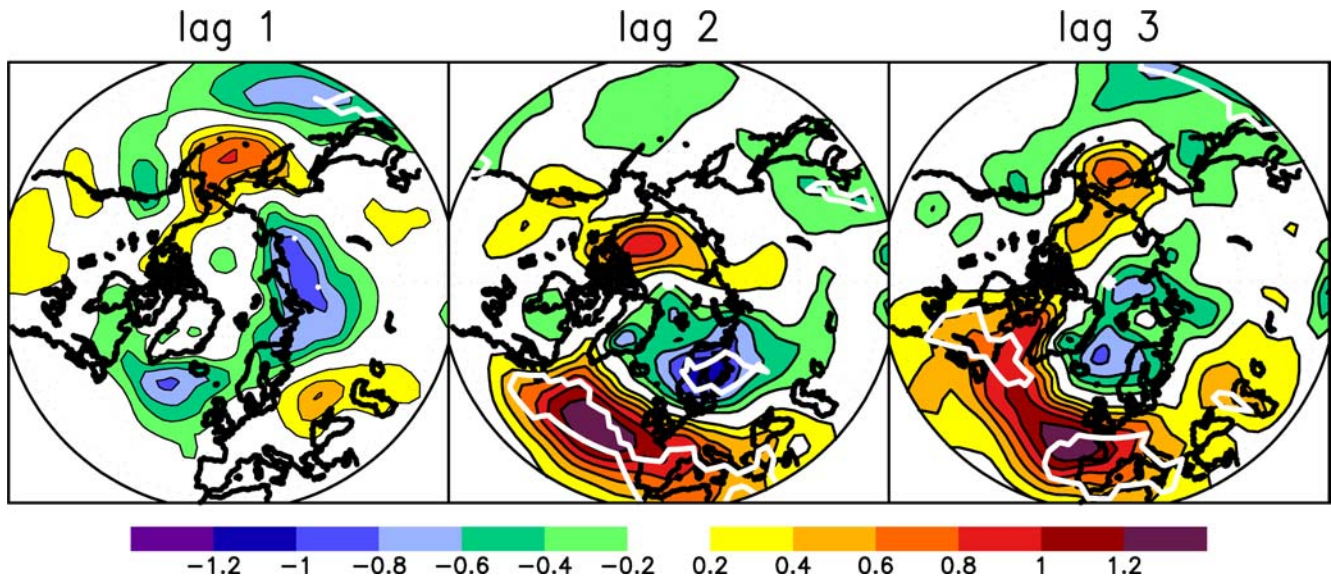
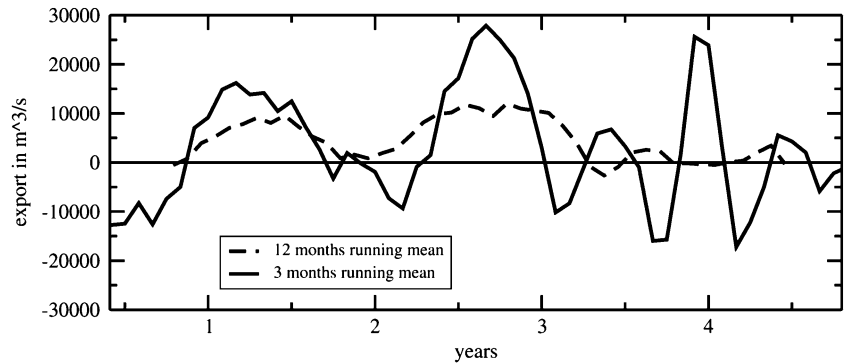


Fig. 15 Annual mean SLP anomalies 1–3 years after the ice export. Mean of the 20 runs. The white line indicates the level of 95% significance

Fig. 16 Fram Strait ice export in m^3/s in the first years after the prescribed ice anomaly. The time axis starts with May in the year with the prescribed ice anomaly



exports accounts to about three-fourths after 1 and 2 years. The probability for anomalies exceeding one standard deviation amounts to slightly more than one-fourths. Similar values are reached for positive salinity anomalies after low ice exports. In 50 from 70 cases of the first and in 58 cases of the second year a positive salinity anomaly occurs, whereas 25 and 26 cases produce large positive anomalies, respectively. Obviously, the fresh water anomaly needs longer to reach the Labrador Sea after low ice exports than after large ice exports. Large ice exports are associated with

northerly winds that accelerate the propagation of the fresh water signal to the south, whereas anomalous southerly winds, associated with low exports, slow down the East Greenland Current. A comparison with the predictability gained from the 1 and 2 years persistence indicates for the first year a similar predictability. For 2 years lead of the ice export, however, the predictability clearly exceeds that of persistence. Using only extreme ice export anomalies of more than one and a half or two standard deviations the prediction for the salinity improves further.

Table 3 Probability (in %) for positive and negative annual salinity anomalies (in standard deviations) in the Labrador Sea 1 and 2 years after large and low ice export. Sixty-eight years with large ice exports and 70 years with low ice exports are used. The probability of the negative and positive persistence is shown in brackets

	Ice > 1 std lag 1 year	Ice > 1 std lag 2 years	Ice < -1 std lag 1 year	Ice < -1 std lag 2 years	Distributional years
$S > 1$	4.4 (3.8)	4.4 (10.1)	35.3 (28.5)	37.1 (22.7)	12.0
$S > 0$	20.6 (23.4)	25.0 (32.3)	71.4 (76.8)	82.9 (61.4)	47.7
$S < 0$	79.4 (76.4)	75.0 (67.7)	28.6 (23.2)	17.1 (38.6)	52.3
$S < -1$	27.9 (22.6)	25.0 (19.3)	2.9 (3.3)	4.3 (6.8)	12.2

Table 4 Same as Table 3 but for 2-m air temperature

	Ice > 1 std lag 1 year	Ice > 1 std lag 2 years	Ice < -1 std lag 1 year	Ice < -1 std lag 2 years	Distributional years
$T > 1$	7.4 (6.3)	8.8 (12.6)	34.3 (29.8)	41.0 (22.6)	16.9
$T > 0$	29.5 (28.8)	30.9 (38.8)	70.0 (67.8)	70.0 (57.3)	48.2
$T < 0$	70.5 (71.2)	69.1 (61.2)	30.0 (32.2)	30.0 (42.7)	51.8
$T < -1$	26.4 (26.3)	25.0 (21.8)	7.1 (4.8)	8.6 (8.7)	16.5

Table 4 presents the same as Table 3 but for 2 m air temperature. The predictability is slightly weaker than for the salinity. Probability values of about 70% are reached for positive (negative) temperature anomalies 1 and 2 years after low (large) ice export anomalies. But the persistence is also slightly weaker than for salinity. Again, the prediction for 2 years in advance, using Fram Strait ice export as predictor, clearly exceeds that of persistence.

An investigation of the probability of seasonal values 1 and 2 years after large and low ice exports shows similar results. The probability for negative temperature anomalies is in the range between 65% and 70% for all seasons after large ice exports and 70–80% after low ice exports. The described process is therefore relevant for the entire year.

6 Summary and conclusions

The impact of the ice export variability through Fram Strait on the atmospheric and oceanic climate in the global coupled AOGCM ECHAM5.0/MPI-OM has been analysed. For the investigations, a 500-year control integration and additional sensitivity experiments have been used. The variability of the ice export depends mainly on the SLP gradient across Fram Strait. Ice thickness anomalies, formed at the coast of Siberian and Chukchi Sea by onshore winds, propagate across the Arctic to Fram Strait in 4–5 years and lead to an increase in ice export. Simultaneously to the increased ice export negative ice thickness anomalies occur at the Siberian coast and take the same way to Fram Strait. This process contributes to the ice export variability and can explain the peak in the spectral analysis at a time period of about 9 years.

To explore the influence of the Fram Strait ice export variability on climate conditions in the northern high latitudes, several oceanic and atmospheric parameters have been analysed after high and low ice export events. After high ice exports, the associated ice/fresh water signal propagates southwards in the East Greenland Current, melts and flows as cold and fresh water into the Labrador Sea. This fresh water anomaly forms a large negative salinity anomaly, 1–2 years after high ice exports. As a consequence oceanic deep convection is reduced or even totally suppressed, which prevents a fast recovery of salinity in the Labrador Sea. In the coupled model, used in this study, the sea ice export through Fram Strait is the main source for the formation of

salinity anomalies in the Labrador Sea, which agrees well with results of Haak et al. (2003) and Häkkinen (1999). However, anomalous fresh water transports through the other three boundaries of the Labrador Sea and local processes contribute to the strength of salinity anomalies in the Labrador Sea.

The cold and fresh water anomaly in the Labrador Sea, after high ice exports, leads to an increase in sea ice concentration and thus to a reduction of the ocean heat release. This has a considerable impact on the atmospheric climate as well. Air temperatures in the Labrador Sea are significantly colder and even the large-scale atmospheric circulation is influenced. Positive SLP anomalies occur over the North Atlantic and parts of Europe, whereas SLP is reduced over the Nordic Seas. Although the size of SLP anomalies are up to 0.6 hPa and so quite small, a comparison with NCEP/NCAR-reanalysis shows that the pattern seems to be robust.

After low ice exports, the entire process proceeds symmetrically.

Sensitivity simulations that prescribe the effect of large ice export events through Fram Strait have been carried out in order to analyse the isolated impact of the associated ice/fresh water signal on climate conditions. In general, the response confirms the results from the analysis of the control integration. Due to the very large fresh water pulse, the resulting anomalies in salinity, temperature and SLP are slightly larger than in the control run. We conclude that the process that leads to the anomalies in atmosphere and ocean is really determined mainly by the fresh water/ice signal, associated with large ice exports. Thus, the initial atmospheric and oceanic conditions play only a minor role.

The results both from the control run and the model simulations show that the Fram Strait ice export explains a considerable amount of the climate variability in the Labrador Sea for the following 2–3 years. To analyse the use of the ice export as predictor for the Labrador Sea, the statistical predictability of 10 m salinity and 2-m air temperature after large positive and negative ice export anomalies has been calculated. The prediction of the sign of the anomaly reaches 75–80% for the salinity and 70–75% for temperature, both 1 and 2 years after high and low ice exports. Predictability for a 2 year lead of ice export clearly exceeds that derived from the assumption of persistence of salinity and temperature anomalies in the Labrador Sea.

Future work will try to further improve the predictability of Labrador Sea climate and to extend the predictability on other parameters.

Acknowledgements This work was supported by the Deutsche Forschungsgemeinschaft through the Sonderforschungsbereich 512. The computations have been performed by the Deutsches Klima Rechenzentrum (DKRZ).

References

- Aagaard K, Carmack E (1989) The role of sea ice and other fresh water in the Arctic circulation. *J Geophys Res* 94:14485–14498
- Alexander M, Bhatt U, Walsh J, Timlin M, Miller J, Scott J (2004) The atmospheric response to realistic Arctic Sea ice anomalies in an AGCM during winter. *J Clim* 17:890–905
- Arfeuille G, Mysak L, Tremblay LB (2000) Simulation of the interannual variability of the wind-driven Arctic sea-ice cover during 1958–1998. *Clim Dyn* 16:107–121
- Belkin I, Levitus S, Antonov J, Malmberg SA (1998) “Great Salinity Anomalies” in the North Atlantic. *Prog Oceanogr* 41:1–68
- Brümmer B, Mueller G, Hober H (2003) A Fram Strait cyclone: properties and impact on ice drift as measured by aircraft and buoys. *J Geophys Res* 1078(D7):6/1–6/13
- Delworth TL, Manabe S, Stouffer RJ (1997) Multidecadal climate variability in the Greenland Sea and surrounding regions: a coupled model study. *Geophys Res Lett* 24 (3):257–260
- Deser C, Walsh J, Timlin M (2000) Arctic sea ice variability in the context of recent atmospheric circulation trends. *J Clim* 13:607–633
- Deser C, Holland M, Reverdin G, Timlin M (2002) Decadal variations in Labrador Sea ice cover and North Atlantic sea surface temperature. *J Geophys Res* 107(C5). 10129/2000JC0000683
- Deser C, Magnusdottir G, Saravanan R, Phillips A (2004) The effects of North Atlantic SST and sea ice anomalies on the winter circulation in CCM3. Part 2: direct and indirect components of the response. *J Clim* 17:2160–2176
- Dickson R, Meincke J, Malmberg SA, Lee A (1988) The “Great Salinity Anomaly” in the northern North Atlantic, 1968–1982. *Prog Oceanogr* 20:103–151
- Dickson R, Osborn T, Hurrell J, Meincke J, Blindheim J, Adlandsvik B, Vinje T, Alekseev G, Maslowski W (2000) The Arctic Ocean response to the North Atlantic oscillation. *J Clim* 13:2671–2696
- Goosse H, Fichefet T, Campin JM (1997) The effects of the water flow through the Canadian Archipelago in a global ice-ocean model. *Geophys Res Lett*. 24(12):1507–1510
- Goosse H, Selten F, Haarsma R, Opsteegh J (2002) A mechanism of decadal variability of the sea-ice volume in the Northern Hemisphere. *Clim Dyn* 19:61–83
- Haak H, Jungclaus J, Mikolajewicz U, Latif M (2003) Formation and propagation of great salinity anomalies. *Geophys Res Lett* 30(9):26/1–26/4
- Hagemann S, Dümenil L (1998) A parameterisation of the lateral waterflow for the global scale. *Clim Dyn* 14(1):17–31
- Hagemann S, Dümenil-Gates L (2003) Improving a subgrid runoff parameterisation scheme for climate models by the use of high resolution data derived from satellite observations. *Clim Dyn* 21(3–4):349–359
- Häkkinen S (1999) A simulation of thermohaline effects of a great salinity anomaly. *J Clim* 6:1781–1795
- Hilmer M, Jung T (2000) Evidence for a recent change in the link between the North Atlantic Oscillation and Arctic sea ice export. *Geophys Res Lett* 27(7):989–992
- Hilmer M, Lemke P (2000) On the Decrease of Arctic Sea Ice Volume. *Geophys Res Lett* 27(22):3751–3754
- Hilmer M, Harder M, Lemke P (1998) Sea ice transport: a highly variable link between Arctic and North Atlantic. *Geophys Res Lett* 25(17):3359–3362
- Houghton R, Visbeck M (2002) Quasi-decadal salinity fluctuations in the Labrador Sea. *J Phys Oceanogr* 32:687–701
- Hurrell J (1995) Decadal trends in the North Atlantic Oscillation: regional temperatures and precipitation. *Science* 269:676–679
- Hurrell J, van Loon H (1997) Decadal variations in climate associated with the North Atlantic Oscillation. *Clim Change* 36:301–326
- Johannessen OM, Myrmehl C, Olsen AM, Hamre T (2002) Ice cover data analysis—Arctic. Technical Report 2, AICSEX
- Jung T, Hilmer M (2001) The link between the North Atlantic Oscillation and Arctic sea ice export. *J Clim* 14(19):3932–3943
- Jungclaus JH, Haak H, Latif M, Mikolajewicz U (2005) Arctic–North Atlantic interactions and multidecadal variability of the meridional overturning circulation. *J Clim* 18(19):4016–4034
- Kalnay E, Kanamitsu M, Kistler R, Collins W, Deaven D, Gandin L, Iredell M, Saha S, White G, Woollen J, Zhu Y, Chelliah M, Ebisuzaki W, Higgins W, Janowiak J, Mo K, Ropelewski C, Wang J, Leetmaa A, Reynolds R, Jenn R, Joseph D (1995) The NCEP/NCAR 40-year reanalysis project. *Bull Am Meteor Soc* 77(3):437–471
- Koeberle C, Gerdes R, Kauker F (1999) Mechanisms determining Fram Strait ice export variability. *ICES-CM 1999/L:25*, 7 pp
- Kwok R, Rothrock DA (1999) Variability of Fram Strait ice flux and North Atlantic Oscillation. *J Geophys Res* 104(C3):5177–5189
- Latif M, Roeckner E, Botzet M, Esch M, Haak H, Jungclaus J, Legutke S, Marsland S, Mikolajewicz U, Mitchell J (2004) Reconstructing monitoring and predicting multidecadal scale changes in the North Atlantic thermohaline circulation with sea surface temperatures. *J Clim* 17(7):1605–1614
- Lazier J (1995) The salinity decrease in the Labrador Sea over the past thirty years. In: Martinson DG, Bryan K, Ghil M, Hall MM, Karl TM, Sarachik ES, Sorooshian S, Talley L (eds) *Natural climate variability on decade-to-century time scales*. National Academic, Washington DC, pp 295–304
- Magnusdottir G, Deser C, Saravanan R (2004) The Effects of North Atlantic SST and sea ice anomalies on the winter circulation in CCM3: Part 1: Main features and storm track characteristics of the response. *J Clim* 17(5):857–876
- Marsland S, Haak H, Jungclaus J, Latif M, Roeske F (2003) The Max-Planck-Institute global ocean/sea ice model with orthogonal curvilinear coordinates. *Ocean Model* 5:91–127
- Murray R, Simmonds I (1995) Responses of climate and cyclones to reductions in Arctic winter sea ice. *J Geophys Res* 100(C3):4791–4806
- Mysak L, Venegas S (1998) Decadal climate oscillations in the Arctic: a new feedback loop for atmosphere-ice-ocean interactions. *Geophys Res Lett* 25(19):3607–3610
- Polyakov I, Johnson M (2000) Arctic decadal and interdecadal variability. *Geophys Res Lett* 27(24):4097–4100
- Power S, Moore D, Post N, Smith N, Kleemann R (1994) Stability of North Atlantic deep water formation in a global ocean general circulation model. *J Phys Oceanogr* 24:904–916
- Proshutinsky A, Johnson M (1997) Two circulation regimes of the wind-driven Arctic Ocean. *J Geophys Res* 102(C6):12493–12514
- Roeckner E, Baeuml G, Bonaventura L, Brokopf R, Esch M, Giorgetta M, Hagemann S, Kirchner I, Kornblueh L, Manzini E, Rhodin A, Schlese U, Schulzweida U, Tompkins A (2003) The atmosphere general circulation model ECHAM5, part 1: Model description. Max-Planck-Institut fuer Meteorologie, Report no. 349, p 127
- Schmith T, Hansen C (2003) Fram Strait ice export during the 19th and 20th centuries: evidence for multidecadal variability. *J Clim* 16(16):2782–2791
- Steele M, Morley R, Ermold W (2001) PHC: a global ocean hydrography with highquality Arctic Ocean. *J Clim* 14:2079–2087
- Terray L, Valcke S, Piacentini A (1998) OASIS 2.2, ocean atmosphere sea ice soil user’s guide and reference manual. Technical Report TR/CGMC/98–05, Centre Europeen de Recherche et de Formation en Calcul Scientifique Avance (CERFACS), Toulouse, France
- Tremblay LB, Mysak L (1998) On the origin and evolution of sea-ice anomalies in the Beaufort-Chukchi Sea. *Clim Dyn* 14:451–460

- Venegas S, Mysak L (2000) Is there a dominant timescale of natural climate variability in the Arctic? *J Clim* 13:3413–3434
- Vinje T (2001) Fram Strait ice fluxes and atmospheric circulation 1950–2000. *J Clim* 14:3508–3517
- Vinje T, Nordlund N, Kvambeck A (1998) Monitoring ice thickness in Fram Strait. *J Geophys Res* 103:10437–10449
- Walsh J, Chapman W (1990) Arctic contribution to upper ocean variability in the North Atlantic. *J Clim* 3(12):1462–1473
- Wang J, Ikeda M (2000) Arctic oscillation and Arctic sea ice oscillation. *Geophys Res Lett* 27(9):1287–1290
- Weatherly J, Briegleb B, Large W, Maslanik J (1998) Sea ice and polar climate in the NCARCSM. *J Clim* 11:1472–1486